

Electronic structure of metal CoSi_2 /insulator CaF_2 superlattice

Koji Akai and Mitsuru Matsuura

Faculty of Engineering, Yamaguchi University, Ube 755-8611, Japan

(Received 5 January 1999; revised manuscript received 24 March 1999)

Electronic structure of metal CoSi_2 /insulator CaF_2 superlattice is studied by the full-potential linearized augmented plane-wave method, based on the density-functional theory. From the comparison of calculated total energies for some atomic configurations in the superlattice interface, it is concluded that the Si layer is in contact with a F layer at the interface. Using this atomic configuration, the band structure and the density of states are calculated: the band structure of the $\text{CoSi}_2/\text{CaF}_2$ superlattices is quite different from the bulks due to electron confinement effects, i.e., the subband structure and highly nested hole sheets appear. Also, band offsets for some energy levels in the superlattice and a transition probability of an electron between two metallic layers under an electric field are calculated. [S0163-1829(99)08231-4]

I. INTRODUCTION

Remarkable progress in crystal-growth techniques, e.g., an epitaxial growth, has brought nanostructure materials such as superlattice, quantum wire, and quantum dot systems. In these artificial materials electronic properties are modified by quantum effects such as a carrier confinement, a resonant tunneling and so on. There are many new electronic devices that have been developed. So far, quantum devices have been studied much in semiconductor heterojunction systems, but research in metal/insulator superlattice systems has been performed very little, nevertheless the latter is considered to be suitable for size reduction and high-speed operation of devices. In metal/insulator superlattice systems electronic states in a metallic layer become those of a quasi-two-dimensional metal, since electrons are confined in the layer by very high potential-barrier of the insulator. By varying an well width and a barrier one, not only electronic structures of a multilayer or a superlattice system but also transport properties are controlled. Thus, it is a good candidate for a new low-dimensional electron system. Up to now ultrathin multilayer systems with metal/insulator heterostructure have been obtained in the combination of silicide or oxide compounds and metals.^{1,2} Using the metal/insulator heterojunction, Asada *et al.* fabricated resonant tunneling diodes and transistors and observed a negative differential resistance.^{3,4}

The electronic structure of these metal/insulator superlattices has not been studied theoretically. Thus, the transport properties have been estimated on the basis of band structures of the bulks. In order to clear electronic and optical properties in metal/insulator superlattices, the information about the electronic structure is necessary. For the electronic structure in superlattice systems the charge transfer between a metallic layer and an insulating layer is important and then effects of charge transfer must be taken into account in the self-consistent calculation of the electronic structure. Including the effects we perform, in the present work, the calculation of the electronic structure of $\text{CoSi}_2/\text{CaF}_2$ superlattice with the use of the full-potential linearized augmented plane-wave (FLAPW) method, based on the density-functional theory.⁵

This paper is organized as follows. In Sec. II, we discuss crystal structures of bulk CoSi_2 and CaF_2 and $\text{CoSi}_2/\text{CaF}_2$ superlattices. In Sec. III, the method of the electronic structure calculation is briefly presented. In Sec. IV, calculated results are shown and are discussed. There, the band structure and the electronic density of states (DOS) of superlattices are presented and the subband-energy is discussed with the comparison of that of the infinite potential model in the quantum well. Also, band offsets are calculated and electron tunneling between metallic layers is discussed. Section V is the summary.

II. CRYSTAL STRUCTURE OF THE SUPERLATTICE

Both bulk CoSi_2 and CaF_2 have the same crystal structures, i.e., the cubic Fluorite structure (O_h^5). Also their lattice constants are very close each other, i.e., 5.356 Å for CoSi_2 and 5.462 Å for CaF_2 .⁶ A $\text{CoSi}_2/\text{CaF}_2$ superlattice has been accumulated on Si(111) substrates by the epitaxial growth technique.¹ The crystal orientation of the growth direction of both CoSi_2 layer and CaF_2 layer is the [111] direction of the fluorite structure, which was confirmed from the high-energy electron diffraction patterns of the superlattice. So far there is not enough available experimental information about all the precise atomic positions, for which we consider as follows. Since the lattice mismatch between CoSi_2 and CaF_2 is small, it is natural to assume that both CoSi_2 and CaF_2 in the superlattice keep the same crystal structure as in the bulk and only the lattice constants are modified. Moreover, both layers in the present superlattice are very thin and then both layers presumably have the same lattice constant, whose value is between 5.356 and 5.462 Å. In the present calculation a lattice constant of CoSi_2 and CaF_2 layers in the superlattice structure is assumed to be the average value of lattice constants of both bulk crystals, i.e., $a = 5.409$ Å, for simplicity.

A unit cell of the cubic fluorite structure is shown in Fig. 1. An open circle shows Co or Ca atom, denoted as M ; a solid circle shows Si or F atom, denoted as X . In the figure, M atoms occupy lattice points of a hexagonal closed packed (hcp) structure, and a basal plane of this structure is parallel to the (111) plane of the fluorite structure. The letters A , B , and C denote three types of the closest-packed layer of the

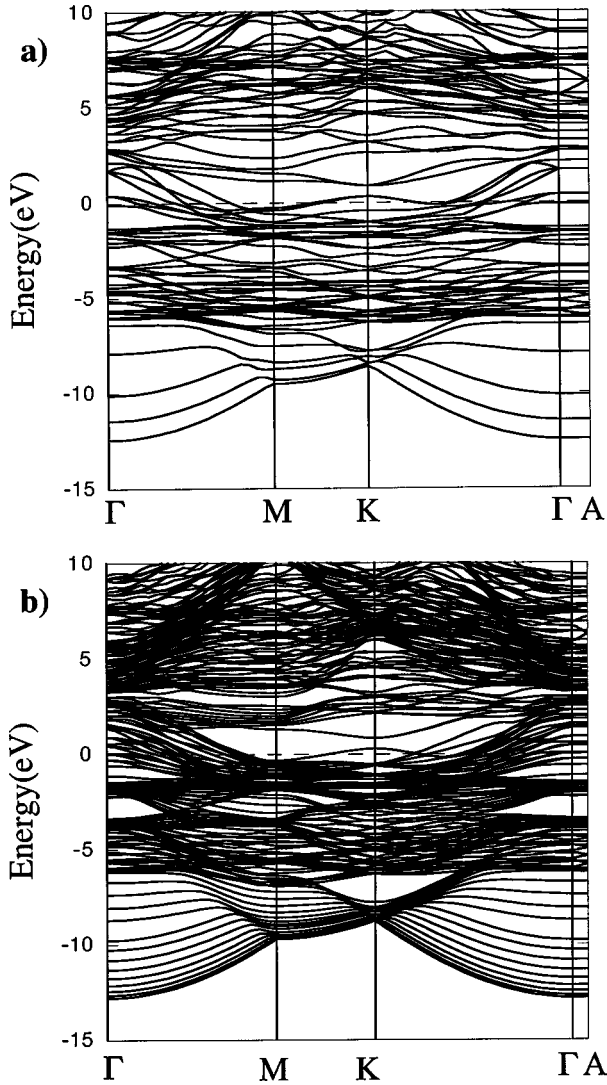


FIG. 2. Band structure of CoSi₂/CaF₂ superlattices: (a) 1-1 type, (b) 3-1 type. The broken line denotes the Fermi energy.

where Ω_i is the i th muffin-tin sphere and N is the total number of the unit cell in the crystal. $\Psi_{n\mathbf{k}}$ defined in Eq. (2) is a Bloch function of the n th band at \mathbf{k} and then $u_{n\mathbf{k}}(\mathbf{r})$ is normalized over a unit cell, i.e., $\int_{\Omega} |u_{n\mathbf{k}}|^2 dV = 1$ (Ω : a unit cell). For the purpose of the comparison the DOS of bulk CoSi₂ and bulk CaF₂ are shown in Figs. 4(a) and 4(b), respectively: the present result for bulk CoSi₂ in Fig. 4(a) agrees with that in the calculation of Ref. 9.

From Figs. 2–4 main features of the electronic structure can be understood as follows. The band structure of the superlattice originates from metallic CoSi₂ and insulating CaF₂ bands. The metallic layer CoSi₂ keeps the metallic character and the insulating layer CaF₂ the insulating one. In the following, we explain this character in more details.

Metallic CoSi₂-like states: The bottom of the conduction band is near -13 eV. In this energy region conduction bands are parabolic in the k_x - k_y plane. These bands are mainly composed from the bonding $3sp$ orbitals of Si atom, which are very wide and Fermi-level-crossing bands in the bulk CoSi₂. The $3d$ bands of Co atom locate around -2 eV, which are narrow and anisotropic. These bands correspond to e_g -like bands of Co in fcc bulk CoSi₂: as the Co site in bulk

CoSi₂ has cubic symmetry, $3d$ states of Co atom split into two type states by the ligand field. Other t_{2g} -like bands of Co are hybridized with $3sp$ orbitals of Si, which become bonding and antibonding wide bands. At the Γ point, these t_{2g} states lie about -4 and 3 eV.

Insulating CaF₂-like states: Bulk CaF₂ is an ionic crystal, and $2p$ states of anion F⁻ are fully occupied and $4s$ states of cation Ca²⁺ are empty. Then bands originated from these states are narrow and the wide-energy gap exist in the bulk because of the small overlapping of wave functions between F⁻ and Ca²⁺. In superlattice systems $2p$ bands of F atom are below the bonding t_{2g} bands of Co atom and lie around -5 eV. The width of their $2p$ bands is about 2.5 eV, which is the same as the bulk value. The empty $4s$ and $3d$ bands of Ca appear around 5 eV.

It should be stressed that there is some hybridization effect of the CoSi₂ and CaF₂ electronic bands. In the energy regions between -6 and -4 eV and between 5 and 7 eV both CoSi₂ and CaF₂ electronic states exist. Then the hybridization occurs and yields the characteristic energy dispersion in the Γ -A direction as seen in Fig. 2, because an electron in insulating layers can move between the layers via the CoSi₂ states. Then the character of these states reflect mainly the insulating CaF₂ states, which can be shown from the behavior of the wave-function amplitude. On the other hand, in the other energy region where there are only the CoSi₂-like states, these states receive the strong confinement effect, which brings the almost no dispersion in the Γ -A direction. This confinement effect is discussed in more details in the following section.

A. Subband structure

One of the characteristic features in superlattice systems is confinement of an electron in metallic layers. The effect causes a subband structure in the electronic states. By comparing Fig. 3 with Fig. 4, the confinement effects are clearly shown; in the energy region between -4 and 4 eV, many spikelike structures appear in the DOS of the superlattice systems and with increasing width of metallic layers the envelop configuration of DOS approaches the DOS of bulk CoSi₂. Moreover, in the low energy below -8 eV many parabolic bands of the $3sp$ orbital of Si appear in Fig. 2 and the stairlike structure of the DOS appears at the same energy region in Fig. 3.

In the low-energy region, we can calculate the energy structure due to the confinement effect with a simple model. In Fig. 3 the solid diamonds denote subband levels at the Γ point, which are calculated from the one-dimensional perfect confinement model of an electron, i.e., the quantum well model with the infinite potential barrier; the Schrödinger equation is written as

$$\left[\frac{p_z^2}{2m} + V_{\text{conf}}(z) \right] \psi_n(z) = E_n \psi_n(z), \quad (10)$$

where $V_{\text{conf}}(z)$ denotes the perfect confinement of an electron in the well with width W , m is a band mass. Then the n th subband energy is obtained from $E_n = (\hbar \pi n / W)^2 / 2m$.

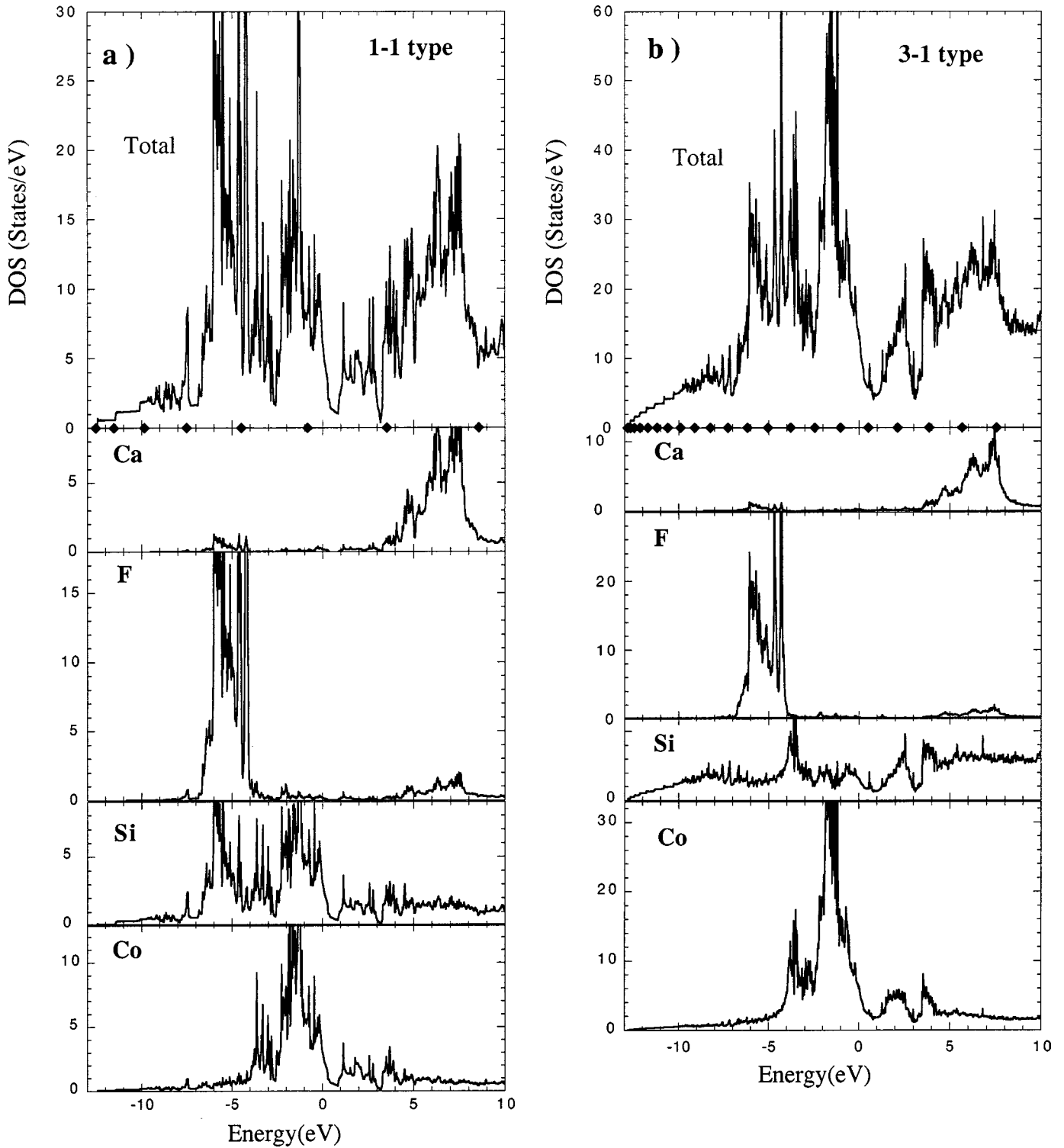


FIG. 3. The total and atomic-decomposed densities of states of the $\text{CoSi}_2/\text{CaF}_2$ superlattice: (a) 1-1 type, (b) 3-1 type. Solid diamonds denote the subband energy at Γ , which is estimated by the one-dimensional perfect confinement model. The Fermi energy is taken to be 0 eV.

In the calculation, we fix the band mass value m of the CoSi_2 $1.6m_0$. The value is calculated from the \sqrt{E} -type DOS near the bottom of the conduction band in the bulk CoSi_2 by the present *ab initio* calculation. The well width is determined to reproduce the energy difference ($\Delta\varepsilon$) between the first and the second parabolic bands of $\text{CoSi}_2/\text{CaF}_2$ superlattices at Γ , in other words the energy differences of the

first and the second kink positions of the stairlike DOS in Fig. 3. Then $W = \hbar \pi \sqrt{3/2m\Delta\varepsilon}$. The determined well width are 0.9 layer in the 1-1 type superlattice and 2.4 layer in the 3-1 type. As shown in Fig. 3, in the low-energy region near the bottom of the parabolic band the calculated energy of some confinement states agrees well with positions of stairlike steps of the DOS, but for higher energy states the agree-

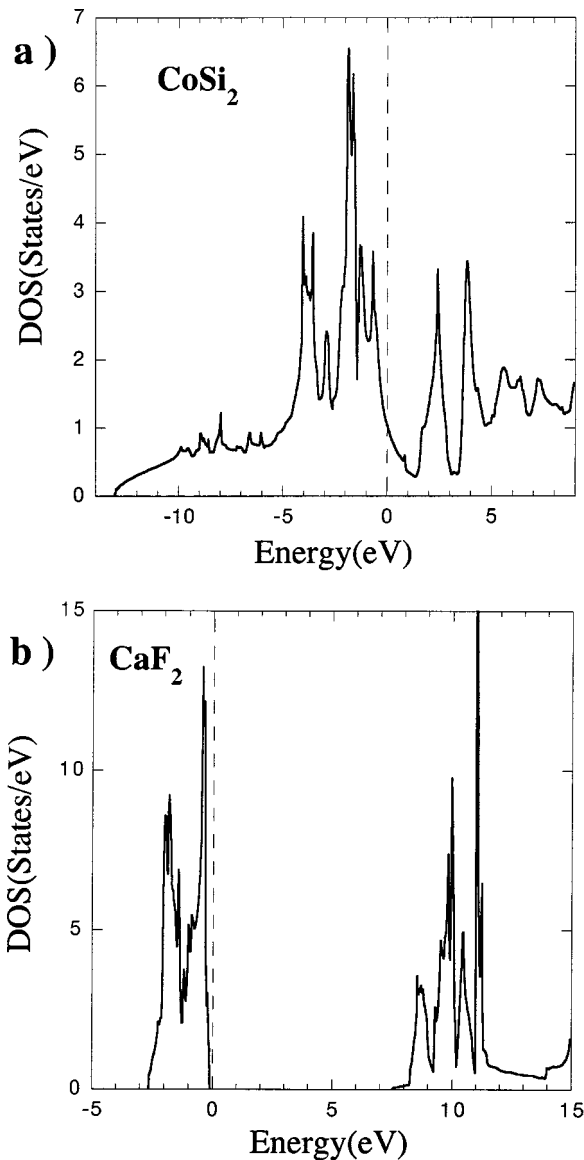


FIG. 4. The DOS of bulk systems: (a) CoSi_2 ($a=5.356 \text{ \AA}$) and (b) CaF_2 ($a=5.462 \text{ \AA}$).

ment is poor. Thus, the simple effective mass approach used to discuss confined electronic states is questionable in the higher energy region.

B. Fermi surface

An interesting feature of $\text{CoSi}_2/\text{CaF}_2$ superlattices is metallic properties, appearing in CoSi_2 layer. Since a metallic CoSi_2 layer is sandwiched between insulating CaF_2 layers, an electron transfers among interlayers by tunneling. Metallic intralayer properties are characterized by Fermi surface structure. The Fermi surface is very complex by the subband structure of the superlattice due to the electron confinement. In order to help the discussion on the Fermi surface of the superlattice, we calculate the electronic structure for CoSi_2 bulk with the hcp lattice instead of that of the fcc lattice. Results of the band structure near the Fermi level and the cross section of the Fermi sphere with the $k_z=0$ plane of the bulk CoSi_2 are shown in Fig. 5. Then bands of the fcc bulk are kept in the first BZ of the hcp lattice. In the bulk seven

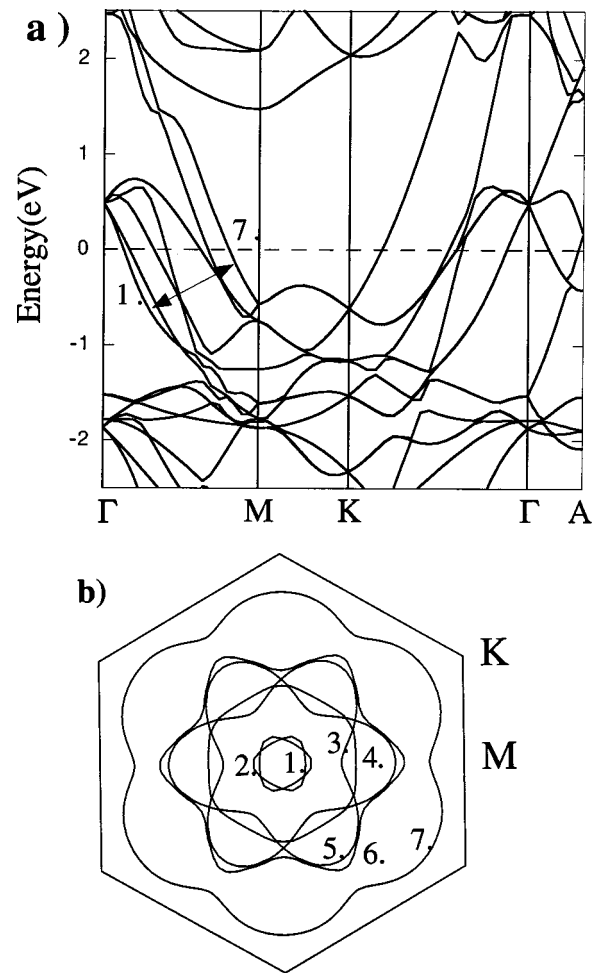


FIG. 5. Band structure (a) and cross section of Fermi spheres with the $k_z=0$ plane (b) in the bulk CoSi_2 with the primitive cell of the hcp lattice. In this band structure seven bands cross Fermi level, which are shown the numbers from 1 to 7.

bands cross the Fermi level as shown in Fig. 5(a), and all their bands bring hole pockets. In Fig. 5(b), Fermi surfaces of these bands are shown. In Figs. 6(a) and 6(b), the cross section of Fermi surfaces in 1-1 type and 3-1 type of superlattices are shown, respectively. A stereoscopic picture of the Fermi surface is easily obtained: the shape of the Fermi surface is cylindrical along the k_z axis, because the band structure between the Γ and the A points is flat near the Fermi energy. In Fig. 6, Fermi surfaces are decomposed into two types: the surface of hole pockets at Γ and one at K . The hole pockets, centered at the Γ point, are made by many subbands due to an electron confinement and correspond to the Fermi holes in the bulk. The other type ones at K do not exist in the bulk CoSi_2 as seen in Fig. 5b, though Fermi surfaces in the bulk expand along the Γ - K line due to the hybridization of $3d$ band of Co. Thus these Fermi holes arise to separate from the large holes at Γ , due to the modification of bands by the superlattice effect.

C. Energy gap

In the present superlattice system the energy gap for an insulating layer can be introduced. Figure 7 shows the site-

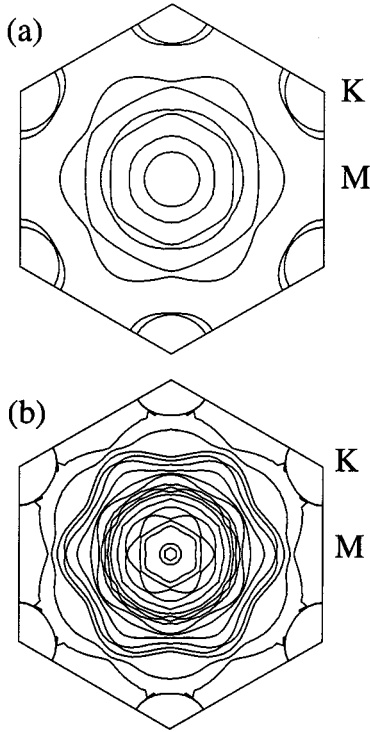


FIG. 6. Cross section of Fermi spheres with the $k_z=0$ plane: (a) the $\text{CoSi}_2/\text{CaF}_2$ superlattice of 1-1 type, (b) 3-1 type.

projected DOS, defined in Eq. (7), for 1-1 type at the Ca and the F sites, which are the nearest and the second nearest-atomic sites from the center of an insulating layer, respectively. The site-projected DOS for 3-1 type is quite similar to that for 1-1 type. From the results the energy gaps of insulating CaF_2 layer in $\text{CoSi}_2/\text{CaF}_2$ superlattices are obtained as 7.9 eV for 1-1 type and 7.6 eV for 3-1 type. These values are compared with the calculated gap, 7.8 eV, in bulk CaF_2

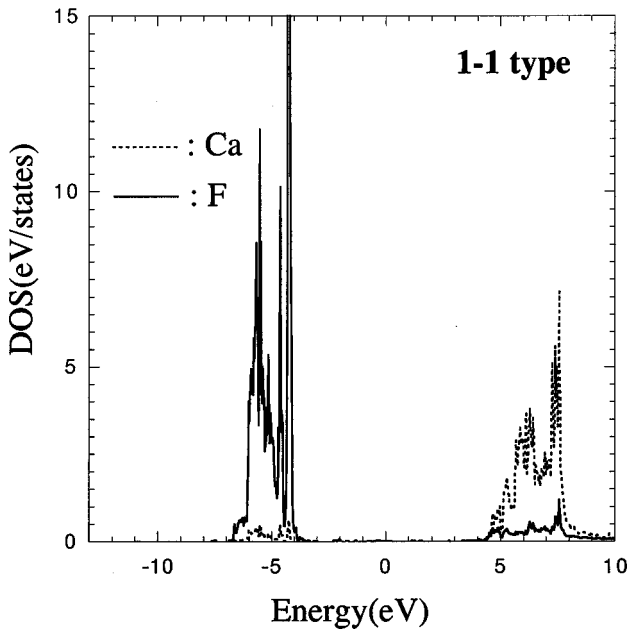


FIG. 7. The site projected densities of states of the 1-1 type $\text{CoSi}_2/\text{CaF}_2$ superlattice, which is defined in Eq. (7).

by the present method. In general, the electronic structure of a superlattice is modified by the electron confinement and the hybridization of energy levels near the interface. But the energy gap of insulating layers in $\text{CoSi}_2/\text{CaF}_2$ superlattices does not change much by the modification. The result is consistent with the electronic structure of the bulk CaF_2 whose conduction bands and valence bands are narrow: these narrow bands yield the small modification of the band gap and the small charge transfer near interfaces.

The magnitude of the band gap from the self-consistent electronic structure calculation is rather small compared to the experimental value. From the far-ultraviolet reflectance spectra of bulk CaF_2 crystals, the band gap has been obtained as 12.1 eV.¹⁰ The disagreement between the theory and the experiment arises from over-screening for a conduction electron in semiconductors or insulators with the usual density-functional method, which can be improved by the inclusion by the self-interaction effects.¹¹ As the screening effects for an conduction electron in a CaF_2 layer by electrons in metallic layers is small, the calculated band gap without the self-interaction effects is not improved for the metal/insulator superlattice.

D. Band offset

Band offsets of semiconductor superlattices have been calculated by the *ab initio* pseudopotential method, based on the density-functional theory.¹² We calculate band offsets in the present system, following the method in Ref. 12. The band offset $\Delta\varepsilon_{\mu\nu}^{AB}$ of A/B superlattices is defined as

$$\Delta\varepsilon_{\mu\nu}^{AB} = \varepsilon_{\mu}^A - \varepsilon_{\nu}^B - \bar{V}_A^{\text{bulk}} + \bar{V}_A^{\text{SL}} + \bar{V}_B^{\text{bulk}} - \bar{V}_B^{\text{SL}}, \quad (11)$$

where ε_{μ}^A and ε_{ν}^B are the eigenenergies of the μ th state with A layer and of the ν th state with B layer, respectively. \bar{V}_A^{SL} and \bar{V}_B^{SL} are the averaged total-potential given in Eq. (3). These potential averages are carried out over a unit cell defined by the A crystal structure or the B crystal structure. These unit cells are taken apart from an interface in order to avoid effects by the charge transfer near the interface. \bar{V}_A^{bulk} and \bar{V}_B^{bulk} are the averaged total potential for the bulks A and B , respectively. Crystal parameters of these bulks are the same as structures of the A -layer part and the B -layer part in the A/B superlattice.

The total potential is singular near nuclear positions. But the difference $\Delta V = V^{\text{SL}} - V^{\text{bulk}}$ does not have singular part, as the potential difference is caused mainly by charge transfer near an interface and difference of the Madelung potential. To make the calculation easier, we use more slowly varying-potential V_p , defined below, instead of the total potential. In the FLAPW method, the potential is expanded by lattice harmonics in muffin-tin spheres and by a Fourier series in the interstitial region. The series is obtained from the electron density in the region. In the interstitial region $V_p(\mathbf{r})$ can be written as

$$V_p(\mathbf{r}) = \frac{1}{\sqrt{\Omega}} \sum_{\mathbf{G} \leq K_{\text{max}}} C(\mathbf{G}) e^{i\mathbf{G} \cdot \mathbf{r}}, \quad (12)$$

where $C(\mathbf{G})$ denotes the Fourier coefficients and Ω is the volume of the system; \mathbf{G} and K_{max} denote the reciprocal

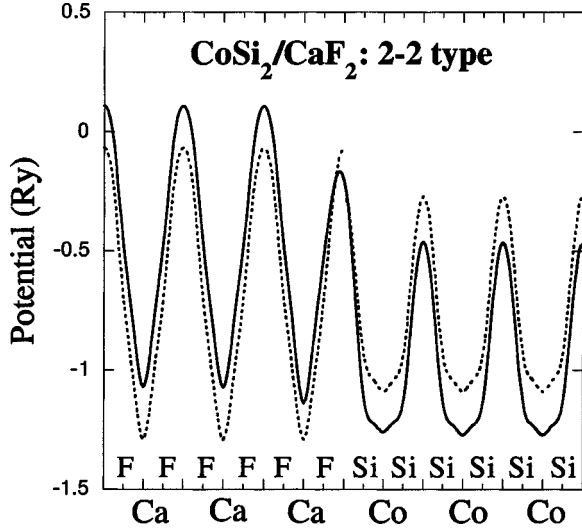


FIG. 8. Potential of the $\text{CoSi}_2/\text{CaF}_2$ superlattice averaged in the plane parallel to the interface. The solid line denotes the 2-2 type superlattice, the broken lines are the potential of the CoSi_2 bulk and of the CaF_2 bulk.

lattice vector and the plane-wave cut off for wave functions, respectively. In the present case K_{max}^{-1} is chosen to be 0.146 \AA^{-1} . $V_s(\mathbf{r}) (\equiv V_{\text{tot}}(\mathbf{r}) - V_p(\mathbf{r}))$ including the singular part of a core potential is expanded by the Fourier series with the reciprocal lattice vector $|\mathbf{G}| \geq K_{\text{max}}$, approximately. Thus, as the difference of the total potential $V_{\text{tot}}(\mathbf{r})$ for superlattice and bulk is slowly varying, the difference of $V_{\text{tot}}(\mathbf{r})$ can be calculated from the difference of $V_p(\mathbf{r})$

$$V^{\text{SL}}(\mathbf{r}) - V^{\text{bulk}}(\mathbf{r}) = \frac{1}{\sqrt{\Omega}} \sum_{\mathbf{G} \leq K_{\text{max}}} D(\mathbf{G}) e^{i\mathbf{G} \cdot \mathbf{r}}, \quad (13)$$

$$= V_p^{\text{SL}}(\mathbf{r}) - V_p^{\text{bulk}}(\mathbf{r}). \quad (14)$$

Figure 8 shows the potential $\bar{V}_p(z)$ defined as:

$$\bar{V}_p(z) = \frac{1}{S} \int \int_{D(z)} V_p(\mathbf{r}) dx dy, \quad (15)$$

where the plane $D(z)$ is parallel to the superlattice interface, S is an area of the interface of the superlattice. The calculation has been performed in the 2-2 type superlattice where both widths of a metallic layer and an insulating layer are 18.7 \AA and thus at the center of each layer the electronic structure of the superlattice become the similar structure on bulks. From Fig. 8, we obtain the potential differences ΔV_{CoSi_2} and ΔV_{CaF_2} as 0.21 and -0.20 Ry, respectively. Then the band diagram of the $\text{CoSi}_2/\text{CaF}_2$ superlattice is obtained and is shown in Fig. 9. As seen in Fig. 9 the band offset between the bottom of the conduction band of CoSi_2 and of CaF_2 is 21.5 eV and the band offset between the bottom of the conduction band of CoSi_2 and the bottom of the valence band of CaF_2 is 6.8 eV . In the calculation the experimental band gap 12.1 eV for CaF_2 has been used.

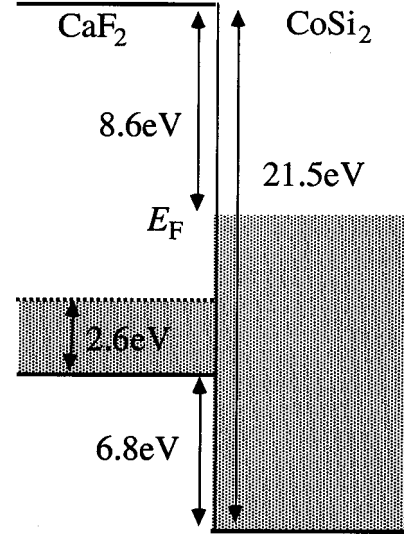


FIG. 9. Energy diagram of the $\text{CoSi}_2/\text{CaF}_2$ superlattice. A thick-solid line denotes the bottom of the conduction or the valence bands and a dotted line denotes the top of the valence band.

E. Electron tunneling

We briefly discuss transport properties of electrons between metallic layers through an insulator layer. As seen in the band diagram near the Fermi energy, electronic states are occupied by the only electrons in metallic CoSi_2 layers and no electronic states are present in insulating CaF_2 layers. Thus the transition rate of an electron between neighboring metallic layers can be calculated from the following expression with use of the present band calculation:

$$w(V) = 2\pi |t|^2 G(V), \quad (16)$$

$$G(V) = \int d\omega \sum_{n, \mathbf{k}_{\parallel}} \delta(\omega - eV - \varepsilon_{n\mathbf{k}_{\parallel}}^A) \times \sum_{n', \mathbf{k}'_{\parallel}} \delta(\omega - \varepsilon_{n'\mathbf{k}'_{\parallel}}^B) \cdot \delta(\mathbf{k}_{\parallel} - \mathbf{k}'_{\parallel}) \times [f(\varepsilon_{n\mathbf{k}_{\parallel}}^A) - f(\varepsilon_{n'\mathbf{k}'_{\parallel}}^B)], \quad (17)$$

where t is a transfer integral between interlayers. In this expression, we neglect dependence of band indices n, n' and wave numbers $\mathbf{k}_{\parallel}, \mathbf{k}'_{\parallel}$ for t , for simplicity. $f(\varepsilon)$ is the Fermi distribution function, \mathbf{k}_{\parallel} is parallel to the heterojunction interface. V is the voltage difference between metallic layers A and B . For $V > 0$, the electrons are transferred from A to B , and vice versa for $V < 0$. Then as the state number within $E_F - eV < \varepsilon_{n\mathbf{k}_{\parallel}}^A < E_F$ or $E_F < \varepsilon_{n'\mathbf{k}'_{\parallel}}^B < E_F + eV$ increases with increasing V , the tunneling current though the insulating layer tends to increase with V ; E_F is the Fermi energy. Exactly speaking, the behavior of the current depends on a shape of the DOS near Fermi level in metallic layers. Figure 10 shows $|G(V)|$ at zero temperature for three different cases: (a) both metallic layers are 1 layer, (b) metallic A layer is 1 layer and metallic B layer is 3 layers; (c) A and B are 2 layer and 2 layer, respectively. About V dependence of $G(V)$ we can roughly divide two regions. First, in the region

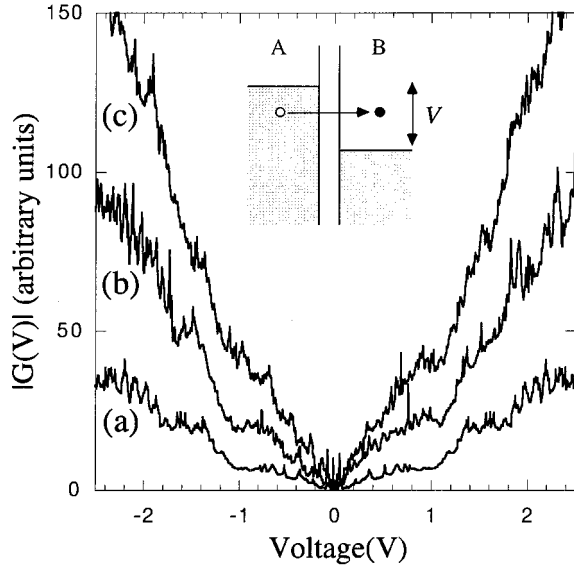


FIG. 10. $|G(\omega)|$, which is proportional to the transfer rate of an electron between metallic layers through the insulating layer: (a) both width of metallic layers are 1 layer, (b) 1 layer and 3 layers, (c) 2 layers and 2 layers. The inset is a schematic picture of metal/insulator/metal-junction under the electric field.

$|V| \lesssim 1$, $G(V)$ has a broad peak and the value is small. Second, in the region $|V| \gtrsim 1$, $G(V)$ increases with $|V|$. These V dependences are consistent with the DOS of the superlattice. As seen in Fig. 3 the Fermi level locates in the high-energy side of the peak due to the $3d$ bands, then until about 1 eV above the Fermi level the DOS decreases monotonously and above about 1 eV the DOS increases. Thus for $|V| \lesssim 1$ an electron transfers from low energy states of $A(B)$ -layer below the Fermi level to high-energy states with the low DOS of $B(A)$ layer: then increase of $|G(V)|$ for the increase of $|V|$ is suppressed. On the other hand for $|V| \gtrsim 1$ there occurs the large tunneling due to the electron transition from the peak of $3d$ bands to other upper band with the high DOS. We think these properties will be observed by measurements of the electrical conductivity.

F. Other discussion

Here we discuss the charge transfer in the superlattice. Figure 11 shows the charge difference between the superlattice and each bulk lattice, which is averaged in the plane parallel to the interface. The charge density of valence electrons is obtained self consistently by the FLAPW method. The charge density in the superlattice is modified in the region of ~ 0.2 layer of the CaF_2 layer and ~ 0.5 layer of the CoSi_2 layer near the interface. In the modified region electrons are removed from CoSi_2 layers to CaF_2 layers, and the interface is the ohmic contact.

Finally, we discuss the effects on the electronic states due to the choice of the lattice constant. In the present paper, we have performed the calculation by using the same lattice constant $a = 5.409 \text{ \AA}$ for both layers, being the average value for the bulks CoSi_2 and CaF_2 . However, in real superlattice systems the electronic structure may be modified from the present results, because the lattice constant of the layers in

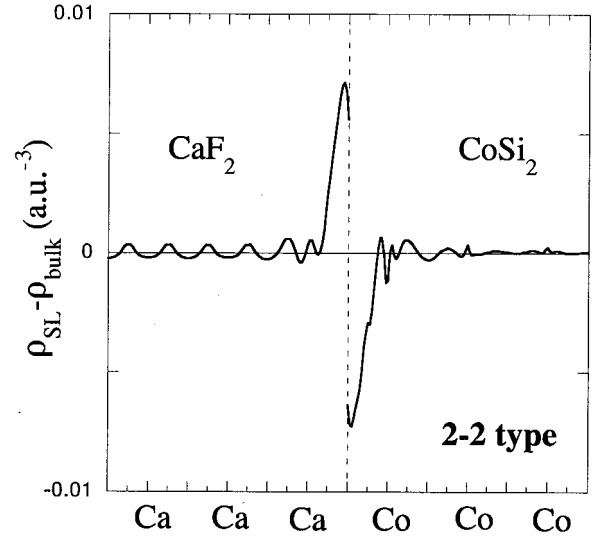


FIG. 11. Planar average of the charge difference between the superlattice and each bulk crystal. The broken line denotes the interface of the $\text{CoSi}_2/\text{CaF}_2$ superlattice.

real superlattices may differ from this simple averaged value. The effect to the electronic structure is estimated by calculating the band structure for the two limiting cases: $a = 5.356 \text{ \AA}$ (bulk CoSi_2) and $a = 5.462 \text{ \AA}$ (bulk CaF_2). The results are very simple: the bandwidth becomes wide or narrow due to the change of the overlapping of wave function in interatomic region for the larger or smaller lattice constant. Then the typical bandwidths $\Delta D = 12.67, 12.50,$ and 12.24 eV are obtained for $a = 5.356, 5.409,$ and 5.462 , respectively, where ΔD is the energy difference between the bottom of the bonding sp -Si band and the Fermi energy. Since the bandwidth changes slightly due to the change of the lattice constants, the electronic structure is modified more slightly, e.g., band offsets shown in Fig. 9 receive only very small correction that is of the order of 0.1 eV or less. Thus the present main results are considered to be valid even when the accurate atomic position in the superlattice is known.

V. SUMMARY

We have calculated the electronic structure of $\text{CoSi}_2/\text{CaF}_2$ superlattices by the FLAPW method based on the density-functional theory. By computing the total energy for several types of the atomic configuration at the interface, it has been concluded that Si layer and F layer are in contact at the $\text{CoSi}_2/\text{CaF}_2$ superlattice interface. Based on the determined interface structure, the band structure and the density of states for the superlattice were calculated. In $\text{CoSi}_2/\text{CaF}_2$ superlattice system typical subband structure appears due to an electron confinement within the metallic layer: the low parabolic band with $3sp$ character of Si yields many states with the subband structure. There the free electron confinement picture works well. In the region near the Fermi level, this picture does not be held, because narrow $3d$ bands lie in the region and hybridize with parabolic sp bands. However, electrons are confined in metallic layers, since CaF_2 layers yield wide-energy gap around Fermi level. In actually, the dispersion of an electron is very small along the k_z axis; the

energy difference between the Γ and the A points is of the order of 0.1 meV for the bands near the Fermi energy, when the insulating-CaF₂ layer is 1 layer, and the Fermi surfaces are cylindrical. As a whole, effects of the subband structure

appear in the DOS of the superlattices clearly; there are stair-like structures of the DOS near the bottom of the conduction band and many sharp peaks corresponding to Van Hove singularities in subbands arise near the Fermi energy.

-
- ¹M. Watanabe, S. Muratake, H. Fujimoto, S. Sakamori, M. Asada, and S. Arai, *Jpn. J. Appl. Phys., Part 2*, **31**, L116 (1992).
- ²T. Kado, *J. Appl. Phys.* **69**, 1393 (1996); **69**, 2208 (1996).
- ³M. Asada, M. Watanabe, T. Suemasu, Y. Kohno, and W. Saitoh, *J. Vac. Sci. Technol. A* **13**, 623 (1995).
- ⁴K. Mori, W. Saitoh, T. Suemasu, Y. Kohno, W. Watanabe, and M. Asada, *Physica B* **227**, 213 (1996).
- ⁵D. J. Singh, *Planewaves, Pseudopotentials and the LAPW Method* (Kluwer Academic, Boston, 1994).
- ⁶R. W. G. Wyckoff, *Crystal Structures*, 2nd ed. (Krieger, Malabar, FL, 1982), Vol. 1.
- ⁷P. Blaha, K. Schwarz, and J. Luitz, WIEN97 (Technical University of Vienna, Vienna, 1997).
- ⁸J. P. Perdew, K. Burke, and M. Ernzerhof, *Phys. Rev. Lett.* **77**, 3865 (1996).
- ⁹L. F. Matthiess and D. R. Hamann, *Phys. Rev. B* **37**, 10 623 (1988).
- ¹⁰G. W. Rubloff, *Phys. Rev. B* **5**, 662 (1972).
- ¹¹F. Gygi and A. Baldereschi, *Phys. Rev. Lett.* **62**, 2160 (1989); R. W. Godby, M. Schlüter, and L. J. Sham, *Phys. Rev. B* **37**, 10 159 (1988).
- ¹²See, for example, C. G. Van de Walle and R. M. Martin, *J. Vac. Sci. Technol. B* **3**, 1256 (1985); M. Murayama and T. Nakayama, *J. Phys. Soc. Jpn.* **61**, 2419 (1992).